



Published in final edited form as:

*Ann Neurol.* 2017 January ; 81(1): 129–141. doi:10.1002/ana.24845.

## Lesions causing freezing of gait localize to a cerebellar functional network

Alfonso Fasano, MD, PhD<sup>1,2,\*</sup>, Simon E. Laganieri, MD<sup>3,\*</sup>, Susy Lam, MSc<sup>4</sup>, and Michael D. Fox, MD, PhD<sup>3,5,6</sup>

<sup>1</sup>Morton and Gloria Shulman Movement Disorders Clinic and the Edmond J. Safra Program in Parkinson's Disease, Toronto Western Hospital and Division of Neurology, University of Toronto, Toronto, Ontario, Canada

<sup>2</sup>Krembil Research Institute, Toronto, Ontario, Canada

<sup>3</sup>Berenson-Allen Center for Noninvasive Brain Stimulation, Division of Cognitive Neurology, Department of Neurology, Harvard Medical School and Beth Israel Deaconess Medical Center, 330 Brookline Ave, Boston, MA, 02215

<sup>4</sup>Institute of Medical Science, Faculty of Medicine, University of Toronto, Ontario, Canada

<sup>5</sup>Athinoula A. Martinos Center for Biomedical Imaging, Massachusetts General Hospital, 149 13<sup>th</sup> Street, Charlestown, MA 02129

<sup>6</sup>Department of Neurology, Massachusetts General Hospital, Harvard Medical School, Mailcode: WACC 8-835, Massachusetts General Hospital, 55 Fruit Street, Boston, MA 02114

### Abstract

**Objective**—Freezing of gait is a disabling symptom in Parkinson's disease and related disorders, but the brain regions involved in symptom generation remain unclear. Here we analyze brain lesions causing acute onset freezing of gait to identify regions causally involved in symptom generation.

**Methods**—Fourteen cases of lesion-induced freezing of gait were identified from the literature and lesions were mapped to a common brain atlas. Because lesion-induced symptoms can come from sites connected to the lesion location, not just the lesion location itself, we also identified brain regions functionally connected to each lesion location. This technique, termed lesion network mapping, has been recently shown to identify regions involved in symptom generation across a variety of lesion-induced disorders.

---

Corresponding author: Dr. Alfonso Fasano, MD, PhD, Associate Professor – Division of Neurology, University of Toronto, Clinician Investigator – Krembil Research Institute, Movement Disorders Centre – Toronto Western Hospital, 399 Bathurst St, 7 Mc412, Toronto, ON Canada M5T 2S8, Phone: +1(416)603-5800 ext 5961, Fax +1 (416) 603-5004, alfonso.fasano@gmail.com.

\*These authors equally contributed to the manuscript and share first authorship

Conflict of Interest: None

**Potential Conflicts of Interest**

None.

**Author Contributions**

Study concept and design (AF, MDF); data acquisition and analysis (SEL, SL); drafting the text or figures (AF, SEL, MDF).

**Results**—Lesion location was heterogeneous and no single region could be considered necessary for symptom generation. However, over 90% (13/14) of lesions were functionally connected to a focal area in the dorsal medial cerebellum. This cerebellar area overlapped previously recognized regions that are activated by locomotor tasks, termed the cerebellar locomotor region. Connectivity to this region was specific to lesions causing freezing of gait compared to lesions causing other movement disorders (hemichorea or asterixis).

**Interpretation**—Lesions causing freezing of gait are located within a common functional network characterized by connectivity to the cerebellar locomotor region. These results based on causal brain lesions complement prior neuroimaging studies in Parkinson's disease patients, advancing our understanding of the brain regions involved in freezing of gait.

### Keywords

Cerebellum; freezing of gait; neuroimaging

---

### Introduction

Freezing of gait (FOG) is an episodic disorder of human locomotion, characterized by sudden and brief episodes of the inability to produce effective forward stepping.<sup>1</sup> The most common cause of FOG is Parkinson's disease (PD), where its prevalence ranges from ~10% in the Hoehn and Yahr stage 1 to more than 90% in stage 4.<sup>2</sup> Although FOG is a common cause of falls and a major determinant of quality of life, the brain regions involved in generating this mysterious motor phenomenon remain unclear.<sup>3</sup>

Neuroimaging studies in PD patients suffering from FOG have identified many structural and functional abnormalities across a variety of brain regions.<sup>4</sup> Implicated regions include components of the motor and premotor networks, executive-attention network, right-sided visuospatial network, caudate nucleus, and locomotor centers in the brainstem.<sup>4</sup> Although highly valuable, it is difficult to determine whether these observed abnormalities are coincidental, causes, consequences, or compensations for FOG symptoms, an important distinction when seeking to identify therapeutic targets.

In the current study, we take an alternative approach towards identifying the neuroanatomical substrate of FOG. Specifically, we focus on cases of acute-onset FOG following focal brain lesions. Lesion-induced FOG symptoms are not identical to all the forms of FOG seen in PD, which is quite heterogeneous.<sup>1,3</sup> However, the main reason to study lesion-induced FOG is that it allows for causal conclusions regarding FOG symptoms and focal neuroanatomical locations. Further, lesion-induced symptoms can potentially lend insight into the neuroanatomical substrate underlying similar symptoms in different diseases.<sup>5,6</sup> The difficulty in studying lesion-induced FOG lies in the fact that these lesions cases are rare and many lesion-induced symptoms fail to localize to a single anatomical location.

To circumvent these problems, we used a recently validated technique termed lesion network mapping to investigate lesion locations causing FOG.<sup>6</sup> This approach involves three steps: 1) transferring the three-dimensional volume of a brain lesion onto a reference brain; 2)

identifying the network of brain regions functionally connected to this lesion volume using a normative connectome dataset; and 3) overlapping lesion-associated networks to identify regions common to a clinical syndrome.<sup>6</sup> The technique is based on the concept of diaschisis and the fact that symptoms can emerge from regions connected to the lesion location, not just the lesion itself.<sup>7</sup> Although this technique is relatively new, it has been used by different research groups to investigate a variety of lesion induced symptoms including visual hallucinations,<sup>6</sup> auditory hallucinations,<sup>6</sup> pain,<sup>6</sup> aphasia,<sup>6</sup> hemichorea,<sup>5</sup> Capgras syndrome,<sup>8</sup> coma,<sup>9</sup> and impaired decision making.<sup>10</sup> In each case, the technique has linked heterogeneous lesions to specific brain regions involved in symptom expression.<sup>6</sup> This technique has also been used to identify the common substrate underlying lesion-induced symptoms when that substrate has no known a priori localization.<sup>5</sup>

## Methods

### Case selection

Case reports of lesion-induced FOG from the existing literature were identified through a systematic search at <http://www.ncbi.nlm.nih.gov/pubmed/> including items published from 1993 up to 2013 with the terms “freezing of gait”, “gait disturbance”, “stroke”, “MRI” and/or “lesion”. Citations from each selected article were cross-referenced. Inclusion criteria were: (1) documented examination describing symptoms of FOG, defined as either marked hesitation with or inability to initiate gait, episodes of abrupt involuntary cessation of locomotion, especially during turns or at transition points, in the absence of significant weakness (2) clearly delineated and circumscribed brain lesions displayed in the article and (3) close temporal relationship between symptom onset and image acquisition. Exclusion criteria included (1) extrinsic compression injuries, (2) significant mass effects, (3) report of whole brain anoxia (4) the presence of competing etiologies for FOG (e.g., idiopathic PD, normal pressure hydrocephalus or neurodegenerative disease), (5) insufficient clinical or radiological detail and (6) poor image quality. Fourteen cases were identified using these criteria (Table 1, Supplemental Table Online).

### Lesion mapping

The lesion location as displayed in the published figure was manually traced onto a reference brain (MNI152 brain, 2 mm × 2 mm, <http://fsl.fmrib.ox.ac.uk/fsldownloads>). Neuroanatomical landmarks were used to ensure the accurate transfer of the lesion location onto the template brain. In cases where more than one lesion was displayed, lesions were mapped together and treated as a single lesion for subsequent analyses. All lesions were mapped true to their laterality. The cohort of 14 lesions is displayed in Figure 1A.

### Lesion network mapping

To investigate the networks associated with FOG lesions, we applied the recently validated technique termed lesion network mapping.<sup>6</sup> This technique involved three steps: 1) the volume of each lesion is transferred to a reference brain 2) the network of brain regions functionally connected to each lesion volume is computed using resting state functional connectivity MRI data from a large cohort of normal participants, and 3) the resulting lesion-network maps are thresholded and overlaid to identify common network sites across

the lesions. Importantly, this technique does not require full 3D lesion volumes and has been shown to work equally well using 2D information from published lesion images.<sup>6</sup>

Our normative resting state functional connectivity MRI dataset consisted of 98 healthy participants (48 male participants, ages  $22 \pm 3.2$  years), part of a larger publicly available dataset.<sup>11</sup> Full methodological and processing details for the normative resting state functional connectivity MRI (rs-fcMRI) dataset are available.<sup>12</sup> Briefly, participants completed one or more rs-fcMRI scans during which they were asked to rest in the scanner with their eyes open. Rs-fcMRI data were processed in accordance with the strategy of Fox et al.<sup>13</sup> as implemented in Van Dijk et al.<sup>14</sup> Functional data were preprocessed to decrease image artifacts and between-slice timing differences. Data were then spatially smoothed using a Gaussian kernel of 6 mm full-width at half-maximum and temporally filtered ( $0.009 \text{ Hz} < f < 0.08 \text{ Hz}$ ). Next, several spurious or nonspecific sources of variance were removed by regression of the following variables: 1) six movement parameters computed by rigid body translation and rotation during preprocessing, 2) mean whole brain signal, 3) mean brain signal within the lateral ventricles, and 4) the mean signal within a deep white matter ROI. Inclusion of the first temporal derivatives of these regressors within the linear model accounted for the time-shifted versions of spurious variance.

Resting state functional connectivity maps were created for each lesion volume using a standard “seed-based” approach. Specifically, the time-course of the blood oxygen level dependent (BOLD) signal within the lesion volume was extracted for each participant in the normative cohort. Correlations between this extracted signal and all other brain voxels were identified and results were combined across participants using a T-test.

### Lesion network overlap

Each of the 14 individual lesion-seeded rs-fcMRI network maps was thresholded at a  $t$  value of positive or negative 2 ( $p < 0.05$ , uncorrected) to identify voxels significantly connected to each lesion location. To ensure that results were not dependent on our choice of threshold we repeated the analysis with  $t$  value thresholds of 3 and 4.25. After applying this statistical threshold, the resulting network maps were binarized and overlapped to identify regions of shared positive or negative correlation (Figure 1B). Regions in this overlap map showing connectivity to 90% (13/14) lesions were identified and center of gravity coordinates for each region were computed.

To ensure that results were not dependent on cases in which the lesion location may be inaccurate (such as tumors, progressive symptoms, or multiple lesions), we repeated our analysis using a subset of 7 cases involving acute-onset, non-progressive FOG following single lesions due to cerebrovascular injury (Case numbers 1,5,7,8,12,13,14).

### Specificity analyses

To evaluate specificity and to control for the possibility that our findings might have been obtained with any set of lesions resulting in abnormal motor control, we compared our FOG lesions to lesions causing two other movement disorders: asterixis and hemichorea-hemiballismus. We chose these two disorders as they are common lesion-induced movement disorders, are readily available in the literature, and were used in a recent publication by our

lab.<sup>5</sup> Hemichorea-hemiballismus cases included 29 patients with lesions located in cortex, STN, putamen, caudate, midbrain, and subcortical white matter. Asterixis cases included 30 patients with lesions located in the thalamus, cortex, brainstem and cerebellum.<sup>15</sup> Full details regarding both of these lesion cohorts have been published previously.<sup>5, 15</sup>

Two statistical approaches were used to compare lesion network mapping results between FOG lesions and control lesions, a Lieberman test and a two-tailed T-test. Both statistical analyses identify voxels significantly more connected to FOG lesion locations than control lesion locations. The difference between these statistical tests is that the Lieberman test classifies voxels in a binary fashion (connected or not) and is more commonly used in lesion analysis,<sup>16</sup> while the t-test takes into account the strength of the connection and is more commonly used in functional neuroimaging. The inclusion of both tests avoids limitations associated with either alone. FOG lesions were compared to the two control cohorts combined (i.e. FOG versus hemichorea-hemiballismus plus asterixis) and each control cohort individually (i.e. FOG vs. hemichorea-hemiballismus and FOG vs. asterixis). Multiple different statistical approaches and comparisons were done to ensure that results were robust to different analytic approaches.

Because the goal of these analyses was to assess the specificity of FOG lesion network mapping results, statistical maps were masked to anatomical regions containing sites of peak FOG network overlap (cerebellum, thalamus, and subcallosal cingulate), using the Harvard-Oxford structural atlas within FSL.

### Overlap with cerebellar locomotor regions

We compared our lesion network mapping results to two separate fMRI studies of human locomotion. The first study compared active vs. passive stepping.<sup>17</sup> The largest peak across the entire brain was located in the left cerebellar vermis (MNI  $x=-8, y=-42, z=-26$ ) with a secondary peak in the right cerebellar vermis ( $x=8, y=-44, z=-26$ ). The second study contrasted mental imagery of locomotion (walking and running) vs. mental imagery of lying.<sup>18</sup> The largest peak across the entire brain was located in a large cluster centered in the bilateral cerebellar vermis with a left-sided peak at (MNI  $x=-6, y=-48, z=-14$ ). Given that secondary peaks in this cluster were not specifically reported, we used MNI  $x=6, y=-48, z=-14$  as the location of the right sided coordinate. Regions of interest were generated by creating 6mm spheres centered at these coordinates. Functional connectivity between these regions of interest and each lesion location was computed using our normative functional connectivity dataset and Pearson's correlation. Resulting  $r$  values were converted to a normal distribution using Fisher's  $r$  to  $z$  transform and statistics were computed using a student's  $t$ -test. Average Fisher  $z$  values were converted back into  $r$  values for display.

### Functional connectivity of the cerebellar overlap site

To identify brain areas functionally connected to our cerebellar overlap site, we used our cerebellar site (thresholded at 13/14) as a seed region to generate a rs-fcMRI map. Peak coordinates in this map were identified using a cluster analysis with a threshold of  $t=6$  (positive correlation only) and two local maxima per cluster (Table 2). This network map is displayed on the cortical surface using CARET<sup>19</sup> and in volume space using FSL.

## Results

Our literature search identified 14 cases of lesion-induced FOG (Figure 1A, Table 1, Supplemental Table Online). There were 3 females, mean age was  $63.6 \pm 15.6$  years (range: 35–83) with a mean follow-up period, when recorded, of 7 months (range: 24hrs-2 years). Lesion etiology was heterogeneous, with ischemic stroke being the most common. Five cases reported response to L-dopa, none of which improved. Lesions were anatomically heterogeneous with seven primarily in the brainstem, three in the basal ganglia, three in the cortex and one in the subcortical white matter. Five lesions were mostly right sided, four were mostly left sided and five were bilateral.

Next, the network associated with each lesion location was computed and areas of network overlap identified (Figure 1B). Despite marked heterogeneity in lesion location, greater than 90% overlap of positively correlated lesion-derived networks occurred in two areas: the bilateral cerebellum (MNI  $x=16$   $y=-44$   $z=-26$ ,  $x=-20$   $y=-44$   $z=-26$ , Figure 2A) and bilateral thalamus (MNI  $x=12$   $y=-20$   $z=4$ ,  $x=-10$   $y=-18$   $z=2$ , Figure 2B). Greater than 90% overlap of negatively correlated networks occurred in the bilateral subcallosal cingulate (MNI  $x=10$   $y=20$   $z=-12$ ,  $x=-14$   $y=22$   $z=-12$ ) (Figure 2C). The cerebellar and thalamic overlap sites were more robust to different thresholds (>50% lesion network overlap even at the highest threshold), than the subcallosal cingulate site (36% network overlap at the highest threshold).

To determine whether this connectivity was specific to lesions causing FOG, we compared networks derived from FOG lesions to networks derived from lesions causing other movement disorders (hemichorea-hemiballismus and asterixis). Voxels in the bilateral dorsal medial cerebellum were significantly more connected to lesions causing FOG than lesions causing other movement disorders using two different statistical approaches (Figure 2D and G,  $P < 0.05$ ). In contrast, voxels in the thalamus and the subcallosal cingulate were non-specific, with no significant difference in connectivity between lesion cohorts (Figure 2E, F, H and I). To ensure that our cerebellar results were robust to choice of control cohort, we also compared FOG lesions to just asterixis lesions (Figure 3A, B) and just hemichorea-hemiballismus lesions (Figure 3C, D). To ensure that our cerebellar results were not driven by FOG lesions with uncertain localization (e.g. tumors, multifocal lesions) we repeated our analysis with a subset of seven single-focus lesions due to acute cerebrovascular events (Figure 3E, F). Results were unchanged across all variations in our statistical or analytic approach.

Because our nodes in the cerebellum seemed close to regions previously identified in neuroimaging studies of locomotion, we created regions of interest based on the coordinates in these prior studies. We found that our lesion locations causing FOG showed significant connectivity to both these cerebellar locomotor regions ( $p < 0.05$ ). Further, this connectivity was significantly greater than that seen with lesions causing either hemichorea-hemiballismus ( $p < 0.001$ , Figure 4A) or asterixis ( $p < 0.05$ , Figure 4A). These results were significant regardless of whether we used a single left sided cerebellar ROI or bilateral ROI generated using the coordinates from Jahn et al.<sup>18</sup> Finally, the spatial distribution of our

lesion network mapping results matched the location of these cerebellar locomotor regions (Figure 4B, C).

Given the emphasis our results placed on this particular location within the cerebellum, we evaluated the connectivity of this site to the rest of the brain (Figure 5A). There was one dominant cortical connection, namely the bilateral leg area of the primary motor cortex, as well as several subcortical sites implicated in motor control (Table 2). As expected, the network of voxels functionally connected to this cerebellar site incorporated the heterogeneous lesion locations resulting in FOG (Figure 5B).

## Discussion

In this study we find that lesions to multiple different brain areas can cause FOG, but these areas are part of a common functional network. Specifically, lesion locations resulting in FOG are functionally connected to a focal area in the dorsal medial cerebellum. This cerebellar area overlaps sites activated in prior studies of human locomotion. These findings complement prior work in other types of FOG, provide insight into the neuroanatomical substrate underlying this disabling symptom, and may have implications for identifying treatment targets.

### Lesion Network Mapping in FOG

Because lesions causing FOG are relatively rare and occur across different brain areas, traditional approaches to lesion mapping have been limited. Our recently validated technique, lesion network mapping, expands lesion analysis by integrating brain connectivity.<sup>5, 6</sup> This technique allows us to determine whether lesion locations share a specific pattern of connectivity, and if so to what region. Regions functionally connected to lesion locations tend to be involved in symptom generation, as previously shown for visual hallucinations, auditory hallucinations, pain, aphasia, hemichorea, and impaired decision making.<sup>5, 6, 10</sup> When applied to lesions causing FOG, this same technique implicates focal areas in the dorsal midline cerebellum that are specific to lesions causing FOG. Because heterogeneous lesion locations causing FOG share connectivity to the dorsal medial cerebellum, and lesions are known to cause dysfunction in connected brain regions,<sup>7</sup> we suggest that this cerebellar region and its associated network may play a role in generating FOG symptoms.

### The role of the cerebellum in locomotion

Bipedal locomotion is a complex process thought to involve a network of cortical and subcortical regions.<sup>20–22</sup> One of these regions, termed the cerebellar locomotor region (CLR), lies at the midline of the cerebellar white matter. Stimulation of this region can induce locomotion in experimental animals.<sup>21,23,24</sup> Neuroimaging studies suggest that a similar CLR may exist in humans. Prior studies have used mental imagery of gait<sup>25</sup> or special foot pedals that allow for active stepping in the MRI scanner.<sup>17</sup> Both approaches identified focal increases in the cerebellum postulated to represent the location of the human CLR.

In the current study, these cerebellar regions previously implicated in locomotion were functionally connected to lesion locations causing FOG. This connectivity was specific to lesions causing FOG versus lesions causing hemichorea or asterixis. Further, the spatial distribution of our lesion network mapping results matched the location of these cerebellar locomotor regions. Collectively, these results suggest that the CLR may play a role in the pathophysiology of FOG in addition to its known role in locomotion.

An interesting question is why, if this cerebellar region is involved in FOG, do patients with cerebellar lesions present with other balance and gait abnormalities but only rarely with FOG. One possibility is that most cerebellar lesions impact a larger area than the focal site identified here, perhaps causing other symptoms that mask or preclude FOG itself. In other words, FOG may require dysfunction of a focal region of the dorsal medial cerebellum, but also require that other regions of the cerebellum remain intact. This type of focal dysfunction may be more likely to occur when lesions occur outside the cerebellum, to sites connected to just one part of the cerebellum. Along these lines, it is worth noting that the only cerebellar lesion in our FOG case series (case #3) is a focal lesion in the vicinity of the cerebellar locomotor area that spares surrounding cerebellar structures.

Another possibility is that preservation (rather than dysfunction) of this CLR node along with lesions to other parts of the locomotor network (defined based on connectivity to the CLR) is responsible for lesion-induced FOG.

### **Will these findings be relevant for PD-related FOG?**

An important question is whether the present results, based on lesion-induced FOG, are relevant for FOG in PD, a much more prevalent and pressing clinical problem. Answering this question requires future work, however there are reasons to think the present results will be relevant.

First, both lesion-induced FOG and PD-related FOG share many clinical features. Both cause an episodic disorder of human locomotion, characterized by sudden and brief episodes of the inability to produce effective forward stepping.<sup>1</sup> However PD-related FOG is heterogeneous and composed of various subtypes.<sup>1, 3</sup> Of these PD subtypes, the one most similar to lesion-induced FOG is likely the “resistant” or “unresponsive” subtype.<sup>3</sup> In this subtype, FOG fails to respond to levodopa, similar to patients with lesion-induced FOG included in the present study (Table 1). As such, while lesion-induced FOG may not match the clinical phenotype of all PD-related FOG subtypes, it is similar to the subtype in greatest need of a treatment.<sup>26</sup>

Second, regions identified in prior lesion network mapping studies have been implicated in generating similar symptoms in different disorders. For example, lesions that cause visual hallucinations are connected to extrastriate visual cortex, a region known to be hyperactive when visual hallucinations are caused by diseases such as macular degeneration.<sup>6</sup> Similarly, lesions causing hemichorea are functionally connected to the posterolateral putamen, a region that becomes hyperintense on MRI in hyperglycemia-induced hemichorea and a region in which atrophy correlates with chorea severity in Huntington’s disease.<sup>5</sup> As such, it



is possible that the dorsal medial cerebellum, implicated here in lesion-induced FOG, will play a role in FOG in other disorders such as PD.

Finally, while the CLR is not featured prominently in most neuroimaging studies of PD-related FOG,<sup>4</sup> several studies have found abnormalities. Specifically, both anatomical connectivity<sup>27–29</sup> and functional connectivity<sup>30</sup> with the CLR have been reported to be abnormal in PD patients with FOG.

The pathophysiology of PD-related FOG is still unclear and 4 main hypotheses have been formulated: the threshold, decoupling, interference and cognitive model.<sup>1</sup> Our findings best support the first two models, which see FOG as a mainly motor problem.<sup>31</sup> However our results also support the interference and cognitive models. Specifically, the cerebellar region identified by our lesion network analysis falls within 5 mm of the peak activation seen with dual-tasking,<sup>32</sup> a manipulation known to exacerbate FOG.<sup>1</sup>

### Treatment targets?

Although some FOG subtypes in PD respond to dopaminergic treatments, FOG is often medication-resistant.<sup>3</sup> This has prompted investigation into brain stimulation treatments. However, the optimal brain stimulation target for FOG remains unknown. Deep brain stimulation of the pedunclopontine nucleus (PPN) has shown some promise, but results have been variable and the role of the PPN in locomotion has been questioned.<sup>20, 22</sup> Interestingly, and in keeping with our findings, in PD patients PPN stimulation increases rCBF in the bilateral cerebellum.<sup>33</sup>

Another stimulation target with some evidence of efficacy in FOG is primary motor cortex, especially the leg area, which has been targeted with both invasive<sup>34</sup> and non-invasive stimulation.<sup>35, 36</sup> Our cerebellar site, identified based on lesions that cause FOG, is also closely connected to the leg area of M1 (Figure 5A). This finding is consistent with the notion that targets of brain stimulation may be brain networks rather than single regions.<sup>37</sup> Whether our cerebellar site and its associated connectivity network will prove valuable for improved targeting of therapeutic brain stimulation for FOG is a testable hypothesis for future work.

### Limitations

Several potential confounds of our lesion network mapping technique have been previously addressed including using a 2D figure to approximate a 3D lesion, using a connectome from a younger cohort to approximate an older cohort, and the impact of different functional connectivity processing techniques. All these variables were found to have little effect on lesion network mapping results.<sup>6</sup> However, there are still important limitations to the current study.

First, due to their rarity lesion cases were retrospectively identified and not directly examined by us. This introduces potential bias based on our search criteria, limits the available clinical and neuroimaging information, and results in a heterogeneous group of lesion cases. However, this heterogeneity should bias us against the current findings of a common functional network. For example, the only FOG lesion that failed to show

connectivity to our midline cerebellar region was a case of lymphoma in which the published image likely failed to capture the full extent of the lesion (case 11). To help mitigate this concern regarding heterogeneity, a sub-analysis with a more homogenous group of FOG lesions was conducted and produced similar results (see Figure 3E, F).

Second, our analysis comes very close to identifying a factor necessary for a lesion to produce FOG, however this should not be interpreted as sufficient. A degree of specificity is present given that two other lesion-induced movement disorders – hemichorea and asterixis – do not share this connectivity, but this is certainly not an exhaustive list of potential comparison conditions. Ideally, we would contrast our FOG lesions with lesions causing a different gait phenotype such as gait ataxia or higher-level gait disorder (HLGD). Unfortunately, there is significant phenotypic overlap between FOG and these conditions. For example, four of our 14 cases of lesion-induced FOG also had some degree of gait ataxia and HLGD patients may have FOG.<sup>38</sup> Even with phenotypic separation, connectivity to our cerebellar site may not be specific for FOG. For example, large lesions causing lower extremity hemiparesis could potentially be connected to our cerebellar site but produce such severe weakness as to preclude FOG. An intact corticospinal tract, relatively intact cerebellum, and perhaps other yet to be identified factors may be required for lesion-induced FOG.

Finally, as discussed in detail above, our analysis was restricted to lesion-induced FOG, which may or may not share the same neuroanatomical substrate with all forms of PD-induced FOG.<sup>3</sup> The applicability of our results to PD-induced FOG require future work.

## Conclusions

Lesions to multiple different brain areas can cause FOG, but these areas are part of a common functional network connected to a focal area in the dorsal medial cerebellum. Our findings based on causative brain lesions complement previous neuroimaging studies focused on FOG correlates in symptomatic patients. These results may guide the development of new therapies for treatment-resistant FOG such as identification of targets for brain stimulation.

## Supplementary Material

Refer to Web version on PubMed Central for supplementary material.

## Acknowledgments

None

## References

1. Nieuwboer A, Giladi N. Characterizing freezing of gait in Parkinson's disease: models of an episodic phenomenon. *Mov Disord.* 2013 Sep 15; 28(11):1509–1519. [PubMed: 24132839]
2. Perez-Lloret S, Negre-Pages L, Damier P, et al. Prevalence, determinants, and effect on quality of life of freezing of gait in Parkinson disease. *JAMA neurology.* 2014 Jul 1; 71(7):884–890. [PubMed: 24839938]

3. Fasano A, Lang AE. Unfreezing of gait in patients with Parkinson's disease. *The Lancet Neurology*. 2015 Jul; 14(7):675–677. [PubMed: 26018594]
4. Fasano A, Herman T, Tessitore A, Strafella AP, Bohnen NI. Neuroimaging of Freezing of Gait. *J Parkinsons Dis*. 2015 Mar 10.
5. Laganieri S, Boes AD, Fox MD. Network localization of hemichorea-hemiballismus. *Neurology*. 2016 May 11.
6. Boes AD, Prasad S, Liu H, et al. Network localization of neurological symptoms from focal brain lesions. *Brain*. 2015 Oct; 138(Pt 10):3061–3075. [PubMed: 26264514]
7. von Monakow, C. Die Localization im Grosshirn und der Abbau der Funktion durch korticale Herde. Wiesbaden, Germany: JF Bergmann; 1914.
8. Darby R, Laganieri S, Pascual-Leone A, Prasad S, Fox MD. Finding the Imposter: Lesions causing delusional misidentifications are characterized by a unique pattern of brain connectivity. *Brain*. 2016 in press.
9. Fischer DB, Boes AD, Demertzi A, et al. A human brain network derived from coma-causing brainstem lesions. *Neurology*. 2016 in press.
10. Sutterer MJ, Bruss J, Boes AD, Voss MW, Bechara A, Tranel D. Canceled connections: Lesion-derived network mapping helps explain differences in performance on a complex decision-making task. *Cortex*. 2016 May;78:131–143.
11. Yeo BT, Krienen FM, Sepulcre J, et al. The organization of the human cerebral cortex estimated by intrinsic functional connectivity. *Journal of neurophysiology*. 2011 Sep; 106(3):1125–1165. [PubMed: 21653723]
12. Fox MD, Buckner RL, White MP, Greicius MD, Pascual-Leone A. Efficacy of transcranial magnetic stimulation targets for depression is related to intrinsic functional connectivity with the subgenual cingulate. *Biol Psychiatry*. 2012 Oct 1; 72(7):595–603. [PubMed: 22658708]
13. Fox MD, Snyder AZ, Vincent JL, Corbetta M, Van Essen DC, Raichle ME. The human brain is intrinsically organized into dynamic, anticorrelated functional networks. *Proc Natl Acad Sci U S A*. 2005 Jul 5; 102(27):9673–9678. [PubMed: 15976020]
14. Van Dijk KR, Hedden T, Venkataraman A, Evans KC, Lazar SW, Buckner RL. Intrinsic functional connectivity as a tool for human connectomics: theory, properties, and optimization. *Journal of neurophysiology*. 2010 Jan; 103(1):297–321. [PubMed: 19889849]
15. Kim JS. Asterixis after unilateral stroke: lesion location of 30 patients. *Neurology*. 2001 Feb 27; 56(4):533–536. [PubMed: 11222802]
16. Rorden C, Karnath HO, Bonilha L. Improving lesion-symptom mapping. *J Cogn Neurosci*. 2007 Jul; 19(7):1081–1088. [PubMed: 17583985]
17. Jaeger L, Marchal-Crespo L, Wolf P, Riener R, Michels L, Kollias S. Brain activation associated with active and passive lower limb stepping. *Front Hum Neurosci*. 2014; 8:828. [PubMed: 25389396]
18. Jahn K, Deutschlander A, Stephan T, et al. Supraspinal locomotor control in quadrupeds and humans. *Prog Brain Res*. 2008; 171:353–362. [PubMed: 18718326]
19. Van Essen DC, Drury HA, Dickson J, Harwell J, Hanlon D, Anderson CH. An integrated software suite for surface-based analyses of cerebral cortex. *J Am Med Inform Assoc*. 2001 Sep-Oct;8(5): 443–459. [PubMed: 11522765]
20. Sherman D, Fuller PM, Marcus J, et al. Anatomical Location of the Mesencephalic Locomotor Region and Its Possible Role in Locomotion, Posture, Cataplexy, and Parkinsonism. *Front Neurol*. 2015; 6:140. [PubMed: 26157418]
21. Takakusaki K, Chiba R, Nozu T, Okumura T. Brainstem control of locomotion and muscle tone with special reference to the role of the mesopontine tegmentum and medullary reticulospinal systems. *J Neural Transm (Vienna)*. 2015 Oct 26.
22. Gut NK, Winn P. The pedunculo-pontine tegmental nucleus-A functional hypothesis from the comparative literature. *Mov Disord*. 2016 May; 31(5):615–624. [PubMed: 26880095]
23. Armstrong DM, Edgley SA. Discharges of interpositus and Purkinje cells of the cat cerebellum during locomotion under different conditions. *The Journal of physiology*. 1988 Jun;400:425–445. [PubMed: 3418533]

24. Mori S, Matsui T, Kuze B, Asanome M, Nakajima K, Matsuyama K. Stimulation of a restricted region in the midline cerebellar white matter evokes coordinated quadrupedal locomotion in the decerebrate cat. *Journal of neurophysiology*. 1999 Jul; 82(1):290–300. [PubMed: 10400958]
25. Jahn K, Deutschlander A, Stephan T, et al. Imaging human supraspinal locomotor centers in brainstem and cerebellum. *Neuroimage*. 2008 Jan 15; 39(2):786–792. [PubMed: 18029199]
26. Espay AJ, Fasano A, van Nuenen BF, Payne MM, Snijders AH, Bloem BR. “On” state freezing of gait in Parkinson disease: a paradoxical levodopa-induced complication. *Neurology*. 2012 Feb 14; 78(7):454–457. [PubMed: 22262741]
27. Schweder PM, Hansen PC, Green AL, Quaghebeur G, Stein J, Aziz TZ. Connectivity of the pedunculopontine nucleus in parkinsonian freezing of gait. *Neuroreport*. 2010 Oct 6; 21(14):914–916. [PubMed: 20729769]
28. Fling BW, Cohen RG, Mancini M, Nutt JG, Fair DA, Horak FB. Asymmetric pedunculopontine network connectivity in parkinsonian patients with freezing of gait. *Brain*. 2013 Aug; 136(Pt 8): 2405–2418. [PubMed: 23824487]
29. Vercruyse S, Leunissen I, Vervoort G, Vandenberghe W, Swinnen S, Nieuwboer A. Microstructural changes in white matter associated with freezing of gait in Parkinson’s disease. *Mov Disord*. 2015 Apr; 30(4):567–576. [PubMed: 25640958]
30. Fling BW, Cohen RG, Mancini M, et al. Functional reorganization of the locomotor network in Parkinson patients with freezing of gait. *PLoS One*. 2014; 9(6):e100291. [PubMed: 24937008]
31. Plotnik M, Giladi N, Hausdorff JM. Bilateral coordination of walking and freezing of gait in Parkinson’s disease. *Eur J Neurosci*. 2008 Apr; 27(8):1999–2006. [PubMed: 18412621]
32. Wu T, Liu J, Hallett M, Zheng Z, Chan P. Cerebellum and integration of neural networks in dual-task processing. *Neuroimage*. 2013 Jan 15; 65:466–475. [PubMed: 23063842]
33. Ballanger B, Lozano AM, Moro E, et al. Cerebral blood flow changes induced by pedunculopontine nucleus stimulation in patients with advanced Parkinson’s disease: a [(15)O] H<sub>2</sub>O PET study. *Human brain mapping*. 2009 Dec; 30(12):3901–3909. [PubMed: 19479730]
34. Fasano A, Piano C, De Simone C, et al. High frequency extradural motor cortex stimulation transiently improves axial symptoms in a patient with Parkinson’s disease. *Mov Disord*. 2008 Oct 15; 23(13):1916–1919. [PubMed: 18709668]
35. Valentino F, Cosentino G, Brighina F, et al. Transcranial direct current stimulation for treatment of freezing of gait: a cross-over study. *Mov Disord*. 2014 Jul; 29(8):1064–1069. [PubMed: 24789677]
36. Kim MS, Hyuk Chang W, Cho JW, et al. Efficacy of cumulative high-frequency rTMS on freezing of gait in Parkinson’s disease. *Restor Neurol Neurosci*. 2015; 33(4):521–530. [PubMed: 26409410]
37. Fox MD, Buckner RL, Liu H, Chakravarty MM, Lozano AM, Pascual-Leone A. Resting-state networks link invasive and noninvasive brain stimulation across diverse psychiatric and neurological diseases. *Proc Natl Acad Sci U S A*. 2014 Oct 14; 111(41):E4367–E4375. [PubMed: 25267639]
38. Giladi N, Huber-Mahlin V, Herman T, Hausdorff JM. Freezing of gait in older adults with high level gait disorders: association with impaired executive function. *J Neural Transm (Vienna)*. 2007; 114(10):1349–1353. [PubMed: 17576512]
39. Robbins MS, Verghese J, Antonietto D. Isolated gait apraxia from an acute unilateral parasagittal lesion. *Clin Neurol Neurosurg*. 2011 Nov; 113(9):782–784. [PubMed: 21880413]
40. Kuo SH, Kenney C, Jankovic J. Bilateral pedunculopontine nuclei strokes presenting as freezing of gait. *Mov Disord*. 2008 Mar 15; 23(4):616–619. [PubMed: 18181207]
41. Ishihara S, Kano O, Ikeda K, Shimokawa R, Kawabe K, Iwasaki Y. Clinicoradiological changes of brain NK/T cell lymphoma manifesting pure akinesia: a case report. *BMC Neurol*. 2011; 11:137. [PubMed: 22047128]
42. Nakajima A, Ueno Y, Shimura H, et al. Acute transient freezing of gait in a patient with posterior reversible encephalopathy syndrome. *BMC Neurol*. 2013; 13:79. [PubMed: 23837548]
43. Robbins MS, Verghese J, Antonietto D. A second case of isolated gait apraxia from an acute unilateral parasagittal lesion. *Clin Neurol Neurosurg*. 2012 Jul; 114(6):823–825.
44. Chung SJ, Im JH, Lee JH, Lee MC. Stuttering and gait disturbance after supplementary motor area seizure. *Mov Disord*. 2004 Sep; 19(9):1106–1109. [PubMed: 15372607]

45. Masdeu JC, Alampur U, Cavaliere R, Tavoulareas G. Astasia and gait failure with damage of the pontomesencephalic locomotor region. *Annals of neurology*. 1994 May; 35(5):619–621. [PubMed: 8179307]
46. Hathout GM, Bhidayasiri R. Midbrain ataxia: an introduction to the mesencephalic locomotor region and the pedunculopontine nucleus. *AJR Am J Roentgenol*. 2005 Mar; 184(3):953–956. [PubMed: 15728623]
47. Krystkowiak P, Delval A, Dujardin K, et al. Gait abnormalities induced by acquired bilateral pallidal lesions: a motion analysis study. *J Neurol*. 2006 May; 253(5):594–600. [PubMed: 16525880]
48. Nadeau SE. Gait apraxia: further clues to localization. *European neurology*. 2007; 58(3):142–145. [PubMed: 17622719]
49. Bhidayasiri R, Hathout G, Cohen SN, Tourtellotte WW. Midbrain ataxia: possible role of the pedunculopontine nucleus in human locomotion. *Cerebrovasc Dis*. 2003; 161:95–96. [PubMed: 12766370]

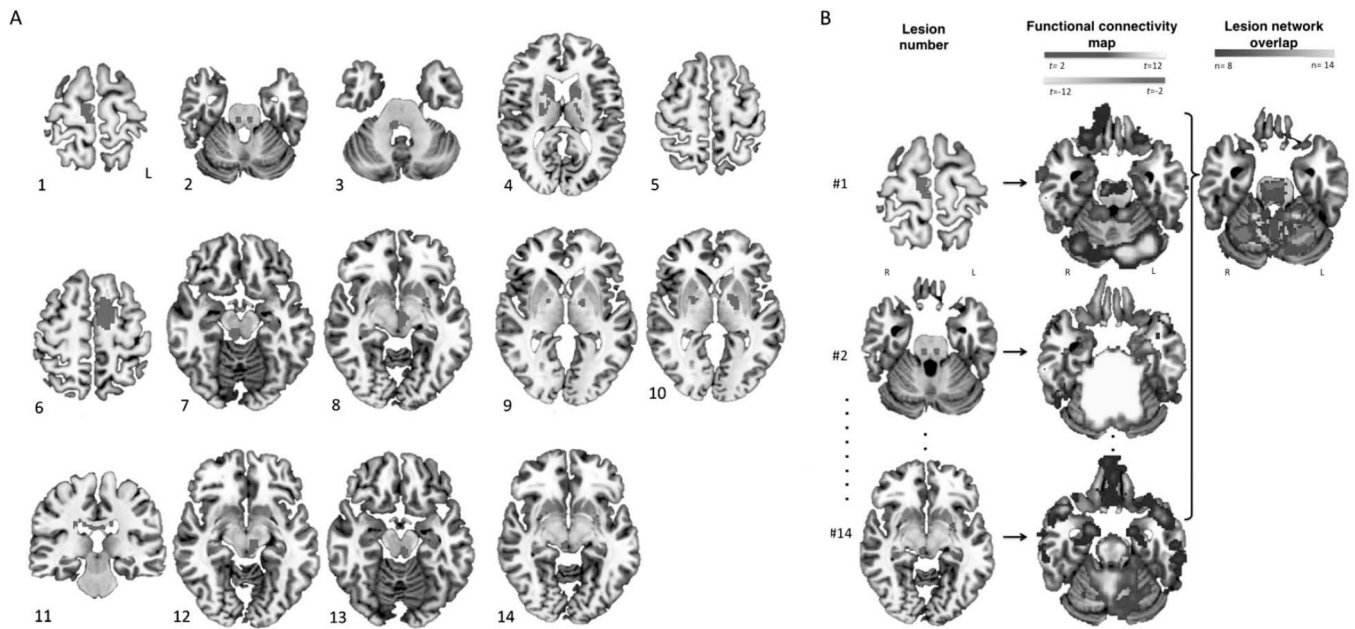


**Figure 1.**

A) Lesion location for 14 cases of lesion-induced FOG, manually traced onto a reference brain (MNI152 template). All lesions were traced true to their laterality, right/left orientation for each lesion as shown on the upper left cross-section. B) Lesion network mapping technique. Each lesion location (left) was used as a seed region to generate a functional connectivity map based on resting state fMRI data from healthy controls (middle). The 14 functional connectivity maps were then overlapped to identify brain regions functionally connected to the greatest number of lesion locations (right).

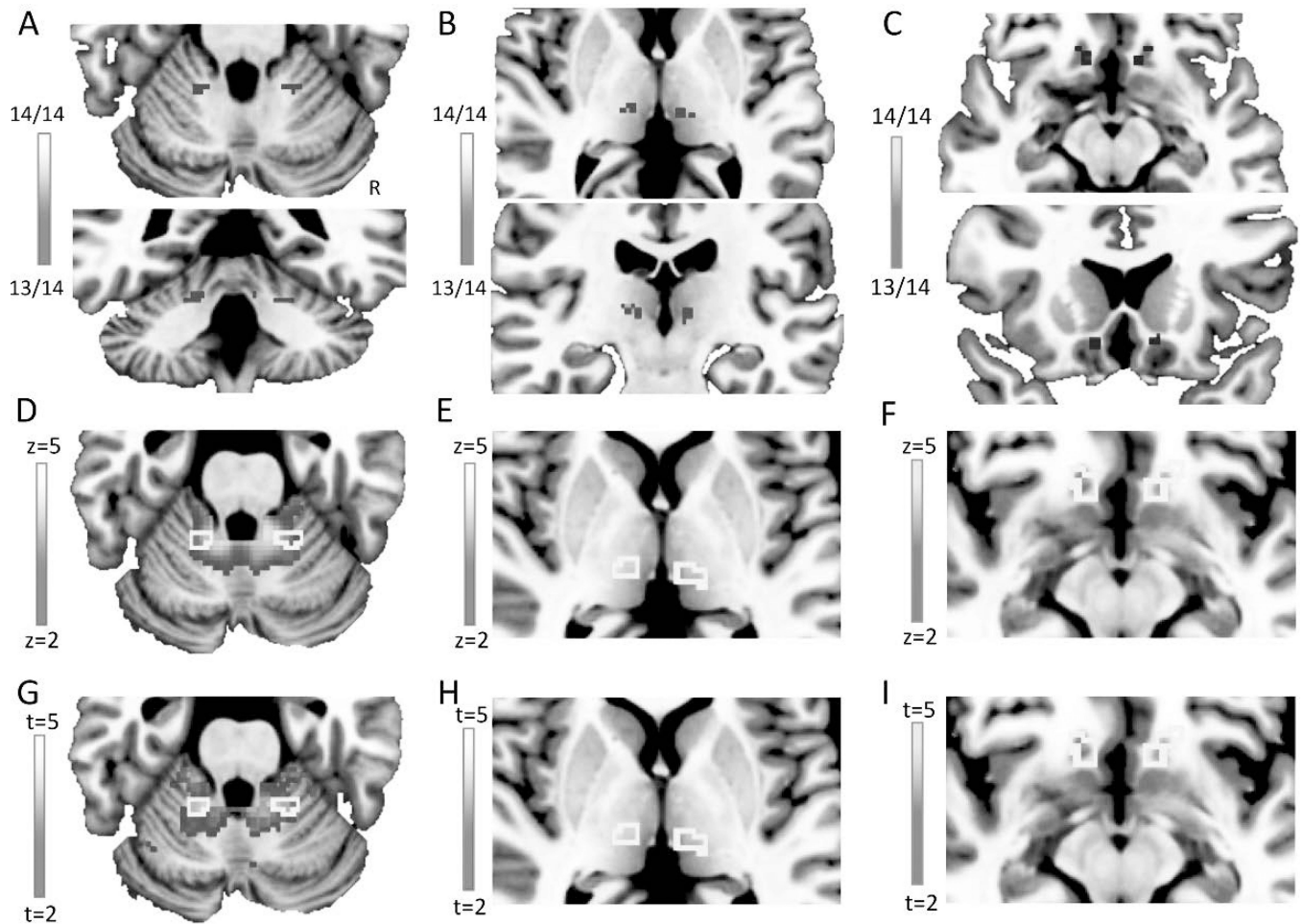


**Figure 2.**

Lesion network mapping results. The vast majority (> 90%) of lesion locations resulting in FOG were positively correlated to sites in the cerebellum (A), thalamus (B) and anti-correlated to sites in the subcallosal cingulate (C). Functional connectivity maps from lesions causing FOG were compared with those causing other movement disorders (asterixis and hemichorea-hemiballismus) using two statistical tests: voxel-wise Leibermeister test (D–F) and unpaired t test (G–I). FOG lesion network overlap sites in the cerebellum, thalamus and subcallosal cingulate (see panels A–C) are outlined in light grey (green in the online version of the figure) for reference. Statistical comparison maps were masked to the cerebellum (D, G), thalamus (E, H) and subcallosal cingulate (F, I), using Harvard-Oxford structural atlases. Connectivity to the dorsal medial cerebellum, but not the thalamus or subcallosal cingulate, is specific to lesions causing FOG.

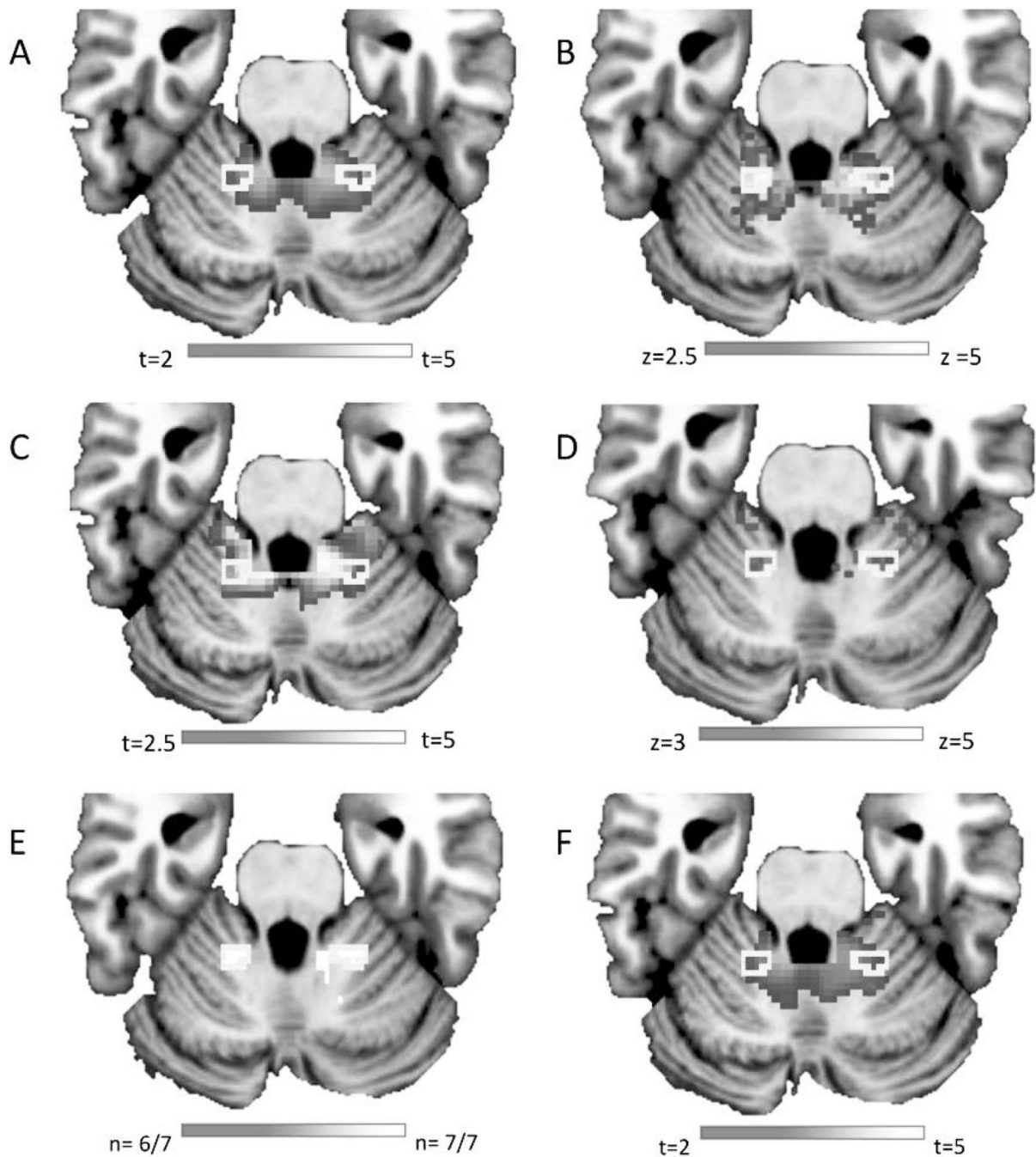


**Figure 3.**

Lesion network mapping results in the cerebellum are robust to several different analysis approaches. Lesion networks derived from FOG lesions are compared to those from asterixis lesions using two statistical tests: unpaired t test (A) or Leibermeister test (B) and to hemichorea-hemiballismus lesions using an unpaired t test (C) or Leibermeister test (D). Lesion network overlap persists in the same location when the inclusion criteria are restricted to cases of acute stroke (E) and remains specific when compared to other movement disorders (asterixis and hemichorea) (F). All images are masked to the



cerebellum. The original FOG network overlap site in the cerebellum (see Figure 2A) is outlined in light grey (green in the online version of the figure) for reference.

Author Manuscript

Author Manuscript

Author Manuscript

Author Manuscript

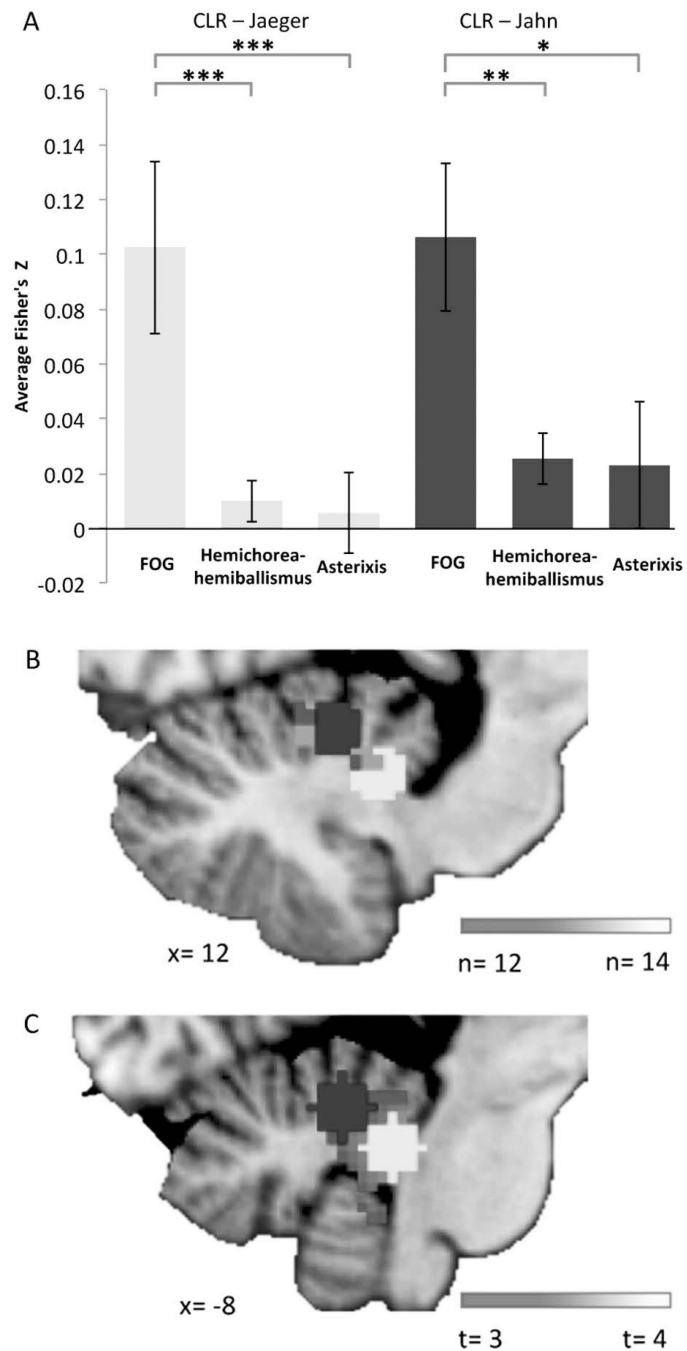


**Figure 4.**

Lesions causing FOG are more connected to cerebellar locomotion regions (CLR) than lesions causing other movement disorders. (A) Mean correlation between lesions causing different movement disorders and one of two putative CLR sites. Topographical display of the FOG lesion network overlap map (B) and voxel-wise t test map comparing FOG to hemichorea-hemiballismus and asterixis (C) are overlaid on two 6mm ROIs centered at the CLR site as outlined by Jahn et al (dark grey, blue in the online version of the figure) and Jaeger et al. (light grey, green in the online version of the figure). T- test map was placed in

front (B) or behind (C) the CLR ROIs for display purposes. \*\*\* $P < 0.001$ , \*\* $P < 0.005$ , \* $P < 0.05$ .

Author Manuscript

Author Manuscript

Author Manuscript

Author Manuscript

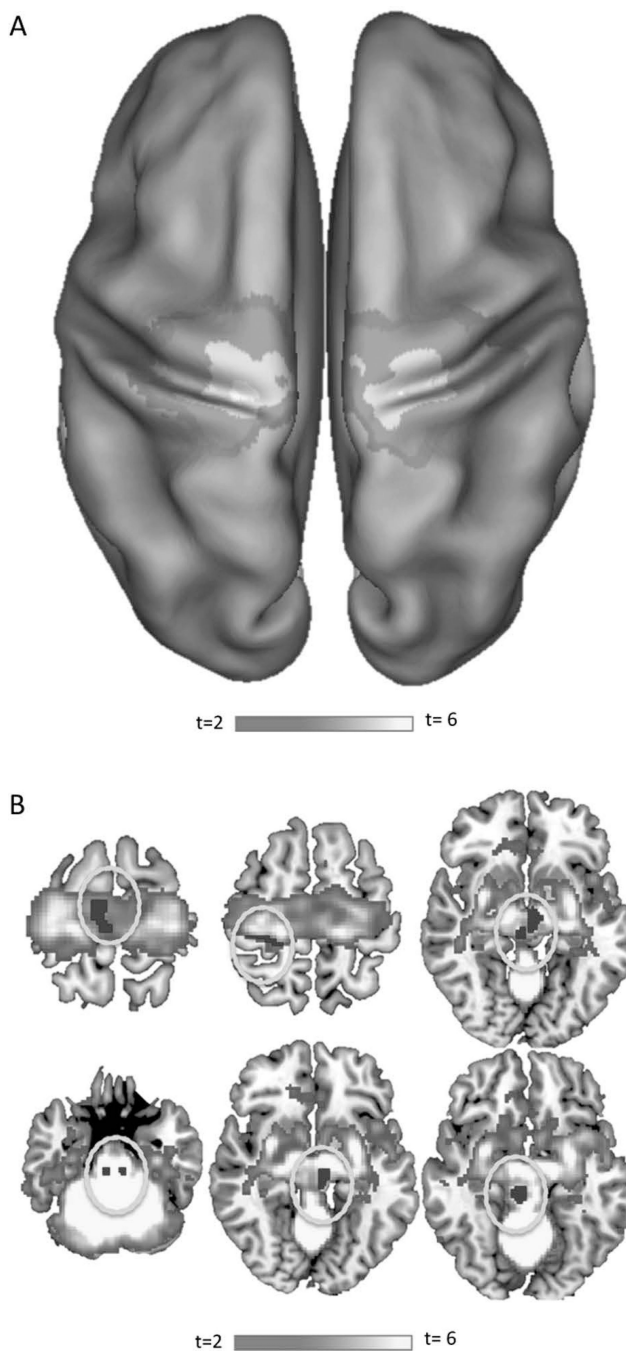


**Figure 5.** Resting-state functional connectivity with the FOG network overlap site in the cerebellum. The map is displayed on the cortical surface using CARET (A) highlighting the bilateral leg area of the primary motor cortex. The same map is displayed on an MNI template brain (B) highlighting subcortical network nodes. Superimposed on the network map in (B) are lesions causing FOG (in dark grey and circled in light grey, blue and circled in green in the online version of the figure).

**Table 1**

Lesional FOG cases included in the analysis.

| Case <sup>ref</sup> | Age/Sex | Underlying Diseases                   | Cause of Lesion                    | Clinical Description   | Follow-up duration | Evolution of Symptoms and treatment effect   | Neuroimaging Findings*   |
|---------------------|---------|---------------------------------------|------------------------------------|--|--------------------|--|--|
| 1 <sup>39</sup>     | 35/F    | Gestational DM                        | Small cortical vein thrombosis     | FOG (especially at doorways and initiating gait), speech impairment, axial bradykinesia, balance disturbance, distal postural tremor                     | 3 months           | Improvement after 72h, able to initiate steps/turns unprompted.  | FLAIR MRI: right parasagittal frontal hyperintensity.  |
| 2 <sup>40</sup>     | 70/M    | HL, depression                        | Ischemic stroke                    | FOG during initiation or turning, intermittent resting leg tremor, distal bradykinesia and rigidity (worse in lower extremities)                         | Unknown            | Progressive worsening of gait. No effect of L-dopa, entacapone, ropinirole and amantadine.   | FLAIR MRI: bilateral brainstem hyperintensities  |
| 3 <sup>41</sup>     | 68/M    | Natural killer cell / T-cell lymphoma | Metastatic disease                 | FOG episodes, start hesitation, short step, forward flexion posture, festination, postural instability   | 2 months           | Ambulation normalized with chemo.  | T2w MRI: hyperintense lesions in the dorsal brainstem/cerebellum                                       |
| 4 <sup>42</sup>     | 43/M    | Chronic renal failure                 | Hemodialysis-induced PRES          | Parkinsonian signs including FOG, bradykinesia, and postural instability   | 4 weeks            | Gradual spontaneous improvement. No effect of L-dopa and amantadine.   | DWI MRI: bilateral basal ganglia hyperintensities (also ADC dark)                                      |
| 5 <sup>43</sup>     | 70/F    | Stiff's disease, HT                   | Traumatic subarachnoid haemorrhage | Difficulty initiating gait, hyperreflexia, widened stance, slow gait and short stride.   | 1 month            | Improvement and normalization over 1 month with physical therapy   | FLAIR MRI: linear hyperintensity (arrow) within the right post-central sulcus                          |
| 6 <sup>44</sup>     | 37/M    | None                                  | Ischemic Stroke / possible seizure | Gait initiation disturbances with paucity of movement, severe bilateral generalized lower extremity bradykinesia with normal motor power and tone.       | 20 days            | Sudden onset gait symptoms 18 months after lesion, 90% improvement over 20 days. No effect of L-dopa   | FLAIR MRI: hyperintensities in the left medial frontal lobe (also ADC dark / DWI bright)               |
| 7 <sup>45</sup>     | 83/F    | HT                                    | Brainstem haemorrhage              | Difficulty initiating gait with significant balance disturbance  | 4 months           | Stable   | T1w MRI: hyperintensity in right brainstem   |
| 8 <sup>46</sup>     | 66/M    | DM, HT                                | Ischemic stroke                    | Marked start hesitation, short irregular unsteady steps, unable to perform tandem gait, ataxia, blurred vision   | 3 days             | Significant gait improvement, ocular findings unchanged  | T2w MRI: hyperintensity in left midbrain tegmentum (also DWI bright)                                   |
| 9 <sup>47</sup>     | 71/M    | HT                                    | Unknown                            | Impaired gait initiation, postural instability with frequent falls, hyponimia, hypokinetic dysarthria, moderate segmental akinesia, cognitive impairment | 6 years            | Progressive gait disorders for 4 years, followed by stable condition for next 2. No effect of L-dopa; slight improvement on amantadine.      | T2w MRI: bilateral "lesions" affecting GPe and GPi   |
| 10 <sup>47</sup>    | 74/M    | HT                                    | Unknown                            | Impaired gait initiation, postural instability, falls, hyponimia and slight hypokinetic dysarthria, cognitive impairment                                 | 5 years            | Progressive gait disorders for 3 years, followed by stable condition for next 2 years. No effect of L-dopa; slight improvement on amantadine | T2w MRI: bilateral focal hyperintensities of GPe and the GPi   |
| 11 <sup>48</sup>    | 76/M    | Primary CNS lymphoma (B-cell type)    | lymphoma                           | Gait ignition difficulty, bilateral paratonia, retropulsion in sitting position, wide gait, shortened steps at turns                                     | Unknown            | Unknown  | Post-contrast T1 MRI: Enhancement of corpus callosum, extending up midline and into parasagittal white |

| Case <sup>ref</sup> | Age/Sex | Underlying Diseases | Cause of Lesion | Clinical Description   | Follow-up duration | Evolution of Symptoms and treatment effect                        | Neuroimaging Findings*   |
|---------------------|---------|---------------------|-----------------|--|--------------------|---|--|
| 12 <sup>46</sup>    | 52/M    | DM, HT              | Ischemic stroke | Gait initiation difficulty, unable to tandem gait, ataxia, blurred vision, short irregular steps with variable amplitude | 6 weeks            | Improvement in gait   | matter bilaterally<br>DWI MRI: Hyperintensity in left dorsal midbrain tegmentum      |
| 13 <sup>49</sup>    | 66/M    | DM, HT              | Ischemic stroke | FOG, truncal and leg ataxia, impaired convergence, upward gaze, skew deviation of eyes, unable to tandem gait            | 3 days             | Gait improved significantly after 3 days (eye problems persisted) | FLAIR MRI: hyperintensity in the left posterior midbrain tegmentum (also DWI bright) |
| 14 <sup>46</sup>    | 80/M    | HT                  | Ischemic stroke | Locomotion initiation difficulty, blurred vision, gait ataxia, broad gait, short steps                                   | 24 hrs             | Ataxia improved slightly  | T2w MRI: Hyperintensity in right dorsal midbrain tegmentum (also DWI bright)         |

\* Abbreviations: images are shown in Supplemental Table Online; ACA: anterior cerebral artery, BPH: benign prostatic hypertrophy, DM: diabetes mellitus, DWI: diffusion weighted images, FLAIR: fluid-attenuated inversion recovery, FOG: freezing of gait, GPe: globus pallidus pars externa, GPi: globus pallidus pars interna, HL: hyperlipidemia, HT: hypertension, MRI: magnetic resonance imaging, MTX: methotrexate, PRES: posterior reversible encephalopathy syndrome, T1w: T1 weighted, T2w: T2 weighted.

Brain regions functionally connected to the FOG network overlap site in the cerebellum. Local maxima in MNI space were identified using a cluster analysis on the voxelwise map shown in Figure 5.

**Table 2**

| cluster # | Local maxima # | t value | x (mm) | y (mm) | z (mm) | Location                             |
|-----------|----------------|---------|--------|--------|--------|--------------------------------------|
| 1         | 1              | 53.1    | 16     | -46    | -26    | Dorsal medial Cerebellum (right)     |
|           | 2              | 50.9    | -18    | -44    | -26    | Dorsal medial Cerebellum (left)      |
| 2         | 1              | 7.97    | 18     | -28    | 64     | Primary motor cortex, medial (right) |
|           | 2              | 6.83    | 28     | -22    | 54     | Primary motor cortex, medial (right) |
| 3         | 1              | 7.55    | -44    | -70    | -46    | Ventral lateral cerebellum (left)    |
|           | 2              | 6.3     | -46    | -56    | -46    | Ventral lateral cerebellum (left)    |
| 4         | 1              | 6.9     | -14    | -28    | 64     | Primary motor cortex, medial (left)  |
|           | 2              | 6.79    | -18    | -28    | 58     | Primary motor cortex, medial (left)  |
| 5         | 1              | 7.97    | 30     | 0      | -10    | Putamen (right)                      |